

# RECOVERY OF NON-FERROUS PARTICLES FROM RECYCLING NEON LAMPS BY MAGNETIC INDUCTION SEPARATOR

NADJIB KADRI<sup>1</sup>, WAFA KRIKA<sup>2</sup>, AHMED NOUR EL ISLAM AYAD<sup>1,\*</sup>, TAHAR ROUIBAH<sup>1</sup>, FEVZI BOZKURT AHMET<sup>3</sup>, ERKAN KADIR<sup>3</sup>, ILIES REZZAG BARA<sup>1</sup>, SHERIF S. M. GHONEIM<sup>4</sup>.

**Keywords:** Induction; Lamps; Lorentz; Magnetic; Neon; Recycle; Separator.

The use of lamps worldwide is rapidly increasing, and the number of broken, burned-out, and defective lamps is very significant, polluting the environment. For this reason, we will address the topic of lamp recycling using magnetic induction technology. This paper presents induction separation by an innovative, improved induction separator design with an important advantage. It extracts aluminum particles from a mixture of waste materials, including non-metallic and non-ferrous particles from broken neon lamps. The induction separator features a single vertical disk rotated by an electric motor. The disk has a series of permanent magnets mounted alternately on its surface. The experimental results of the separation process achieved through an induction separator exhibit a high purity level, boasting a 100% separation efficiency, surpassing the performance of previous separators. These findings substantiate the validity of employing the induction separator to recycle conductive materials.

## 1. INTRODUCTION

The use of fluorescent lamps worldwide has experienced significant growth due to several advantages, including strict regulations, economic factors, and energy efficiency [1,2]. However, the high number of burned-out and broken lamps necessitates recycling and end-of-life disposal efforts [1,2].

Fluorescent lamps contain various ferrous and non-ferrous materials, glass, and chemical gases (mercury, lead, and yttrium) [3,4]. The recycling industry for lamps offers several advantages, such as minimizing chemical risks (environmental pollution), reducing the risk of injuries from glass, and minimizing waste [4]. Lamp recycling can be done in several ways. Magnetic induction separation is the simplest and most efficient technique for reclaiming non-ferrous metals from burned-out lamps. This technique allows for the valorization of raw materials after removing chemical contaminants. [2,4].

Nonferrous particles can be recovered from waste with various types of eddy current separation, each characterized by its shape, orientation, configuration, and several other properties [5]. A drum, disk (with permanent magnets), and an electromagnet (coil) in rotation or static state can generate the magnetic field in a separator [5,6]. Characterizing the eddy current separation process by simulation and experiment studies helps to improve the separation rate and purity of small and big particles [7,8].

There are several studies on recycling lamps and their plastic, glass, and chemical components. For instance, one study explores the use of electrodynamic forces to separate plastic components in LED lamps [4]. The composition of the chemical gases effect is detailed in the research of exposure to workplace hazards within the French fluorescent lamp recycling industry [3]. The reuse of glass extracted from lamp recycling has been examined and evaluated through various approaches [1]. Examining the LED lamp recycling process is undertaken with a focus on the 10 R strategy. This assessment aims to rectify this shortfall by appraising current approaches through the lens of the 10 R principles, which include refusal, reevaluation, innovative thinking, reuse, rejuvenation, refurbishment, fresh production, repurposing, recycling, and resource reclamation [2].

This study will use a magnetic induction separator to separate

particles from a neon lamp containing non-metallic glass and non-ferrous aluminum. The non-ferrous recovery particles from the lamps depend on several factors, such as particle size, velocity, mixture concentration, and separator characteristics.

To better characterize our magnetic induction separator, we will simulate it through a three-dimensional finite element analysis to visualize the concentration of magnetic field lines around the disk and the induced current in ferrous particles near the separator. Experimental trials will be conducted to assess the recovery rate and the purity of separation in each collector.

The primary objectives are to maximize material recovery, minimize raw material consumption, and valorize the material while reducing environmental waste.

Figure 1 depicts a photograph of waste containing a quantity of burnt-out neon lamps discarded at the end of their life – an actual photo of waste in the trash taken at Hassiba Benbouali University Chlef Algeria, 2022.



Fig. 1– Neon Lamps broken in waste.

## 2. DESCRIPTIVE DIAGRAM OF MAGNETIC EDDY CURRENT SEPARATOR

Figure 2 illustrates the principle of separating a mixture of glass and aluminum. The mixture falls through an inclined vibrating conveyor. At the same time, the rotation of a permanent magnet disk generates an alternating magnetic field at a specific frequency (an electric motor controls the rotational speed). The primary field induces a secondary field in non-ferrous particles, resulting in induced currents and repulsion due to the Lorentz force at a certain distance. In contrast, non-metallic particles will fall under the influence of gravity.

<sup>1</sup> Department of Electrical Engineering, Kasdi Merbah University, Ouargla, 30000, Algeria

<sup>2</sup> Automatic Department, Djilali Liabes University of Sidi Bel Abbas, APELEC Laboratory, 22000, Algeria

<sup>3,\*</sup> Mechatronics Engineering Department, Yildiz Technical University, Yildiz Campus, Besiktas, Istanbul, Turkey

<sup>4</sup> Department of Electrical Engineering, College of Engineering, Taif University, P.O. Box 11099, Taif 21944, Saudi Arabia

E-mails: kadri.nadjib@univ-ouargla.dz, wafa.krika@univ-sba.dz, ayad.ahmed@univ-ouargla.dz (correspondence)

hocine\_pg@yahoo.fr, bozkurt@yildiz.edu.tr, kerkan@yildiz.edu.tr, ilyesrezzag@gmail.com, s.ghoneim@tu.edu.sa

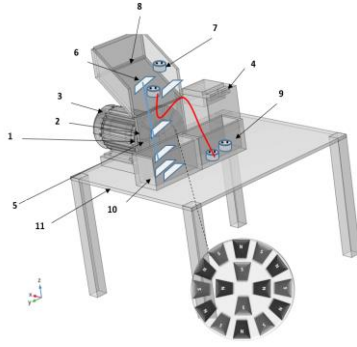


Fig. 2– Geometry of induction magnetic separator.  
 1 – Single vertical disk (surrounded by surface permanent magnets),  
 2 – Permanent magnets, 3 – Rotate motor, 4 – Speed Controller,  
 5 – Plexiglas plaque, 6 – Non-ferrous Particles, 7 – Glass Particles,  
 8 – Inclined feeder, 9 – Collector 1, 10 – Collector 2, 11 – Metallic table.

Fig. 2– Geometry of induction magnetic separator.

Figure 2 illustrates the principle of separating a mixture of glass and aluminum. The mixture falls through an inclined vibrating conveyor. At the same time, the rotation of a permanent magnet disk generates an alternating magnetic field at a specific frequency (an electric motor controls the rotational speed). The primary field induces a secondary field in non-ferrous particles, resulting in induced currents and repulsion due to the Lorentz force at a certain distance. In contrast, non-metallic particles will fall under the influence of gravity.

### 3. MATHEMATICAL MODEL

Electromagnetic modeling integrates Ampere's and Faraday's laws, forming the Maxwell system equations. This system constitutes a local partial differential model within electromagnetism [9,10]:

$$\text{Ampere's Law} \quad \vec{\nabla} \times \vec{H} = \vec{J} + \frac{\partial \vec{D}}{\partial t} \quad (1)$$

$$\text{Faraday's Law} \quad \vec{\nabla} \times \vec{E} = -\frac{\partial \vec{B}}{\partial t} \quad (2)$$

$$\text{Gauss' Law} \quad \nabla \cdot \vec{D} = \rho \quad (3)$$

$$\text{Gauss' Magnetism Law} \quad \nabla \cdot \vec{B} = 0, \quad (4)$$

where  $\vec{B}$  is the magnetic flux density,  $\vec{H}$  – the magnetic excitation field,  $\vec{J}$  – the current density,  $\vec{E}$  – the electric field,  $\rho$  – the volume density of electric charge, and  $\vec{D}$  – the electric induction.

Electromagnetic modeling involves establishing relationships that describe the properties of the medium under consideration, including permanent magnets, steel, air, and non-ferrous particles [10,11]

$$\vec{B} = \mu \vec{H} + \vec{M}, \quad (5)$$

$$\vec{J} = \sigma(\vec{E} + \vec{E}_{ext}) = \sigma \vec{E} + \vec{J}_{ext}, \quad (6)$$

where  $\mu$  is the magnetic permeability,  $\sigma$  is the electrical conductivity,  $\vec{J}_{ext}$ ,  $\vec{E}_{ext}$  and  $\vec{M}$  are the current density imposed from the exterior, the electric field, and respectively the magnetization of the permanent magnets [11].

#### A. Motion consideration

The moving particles with initial velocity  $\vec{v}$  can be added to the Equation (6)

$$\vec{J} = \sigma \vec{E} + \vec{J}_{ext} + \sigma(\vec{v} \times \vec{B}). \quad (7)$$

We compute the rotating magnetic field (dynamic) to

separate conductive (non-ferrous) particles. Furthermore, we considered the effects of induced currents caused by changes in the magnetic field and the motion of conductive particles [9,11]. To accomplish this, we repeatedly solved the equation for each rotation increment of the disk:

$$\vec{\nabla} \left( \frac{1}{\mu} \nabla \times \vec{A} \right) + \sigma \left( \frac{\partial \vec{A}}{\partial t} - \vec{v}_p \times \vec{B} \right) = \frac{1}{\mu} (\nabla \times \vec{B}_r). \quad (8)$$

In this context,  $\vec{A}$  represents the magnetic vector potential,  $\vec{B}$  stands for the magnetic flux density at the location of the particle,  $\vec{B}_r$  represents the remaining magnetic flux density generated by the magnets,  $\mu$  denotes the magnetic permeability, and  $\sigma$  and  $\vec{v}$ , respectively refer to the electrical conductivity of the particle and its velocity of displacement. The magnetic ejection force exerted on a magnetic particle is given by:

$$\vec{F}_m = \mu_0 \int_{v_p} (\vec{M} \cdot \nabla) \vec{H} dv. \quad (9)$$

In the given technical context, we have the magnetic field strength represented by  $\vec{H}$  at the particle location, particle magnetization is denoted as  $\vec{M}$ , ( $\mu_0$ ): the vacuum magnetic permeability and ( $v_p$ ): the particle volume. The eddy current in the non-ferrous particle due to the variable applied field is expressed as follows:

$$\vec{J}_F = -\sigma \frac{\partial \vec{A}}{\partial t}. \quad (10)$$

The particle's movement within the magnetic field results in the creation of an additional component of the eddy currents, which can be expressed as:

$$\vec{J}_{Fa} = \sigma(\vec{v}_p \times \vec{B}) \quad (11)$$

The force exerted on the conductive particle is determined as follows:

$$\vec{F} = \left( -\sigma \left( \frac{\partial \vec{A}}{\partial t} - \vec{v}_p \times \vec{B} \right) \times \vec{B} \right). \quad (12)$$

The trajectory of a repulsed non-ferrous particle computation depends on the resolution of the dynamic equation provided by

$$\sum \vec{F} = m_p \frac{\partial \vec{v}_p}{\partial t} \quad (13)$$

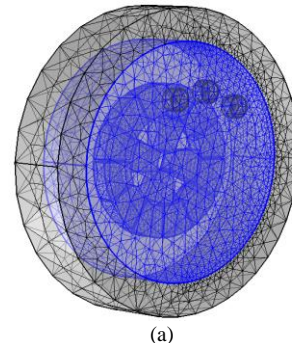
where  $m_p$  represents the mass of the particle, while  $F$  the combined result of the applied forces [9,12].

To solve the previous equation of motion, we considered the Lorentz force law and gravity.

### 4. 3D SIMULATION OF INDUCTION SEPARATOR WITH SINGLE VERTICAL DISK

#### FINITE ELEMENT ANALYSIS

The finite element method is used to compute parameters accurately (to solve complex problems and geometry, nonlinear parameters) and obtain a more approximate design of a single disk of eddy current separator [12]. The rotational separator is studied in a dynamic state with time variation; this behavior is based on moving a mesh using a partial differential equation into a numeric solver (Fig. 3a).



(a)

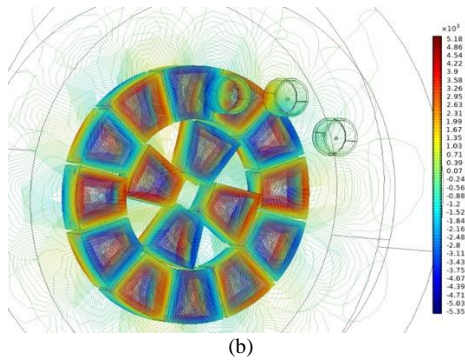


Fig. 3 – The presence of multiple non-ferrous particles: (a) Meshing of induction magnetic separator; (b) Magnetic distribution lines around the separator and particles.

Figure 3 illustrates the magnetic scalar potential distribution lines in proximity and around a vertical single disk and particles generated by permanent magnets, considering the coupling in a magnetodynamic state.

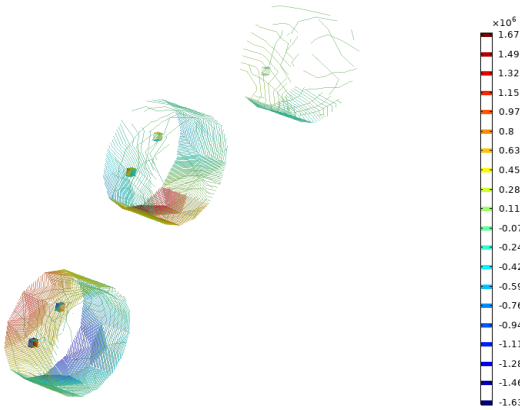


Fig. 4 – Induced current in four non-ferrous particles.

The eddy current contour concentration in aluminum particles changes because of position, shape of non-ferrous particles, and disk speed (Fig. 4).

Table 1

Influence of speed variation on electromechanics' parameters

Speed (Rpm)	$J$ (A/m <sup>2</sup> )	$F$ (N)
300	3e5	1.44
600	3.6e5	1.73
900	4e5	1.92
1200	5e5	2.4
1500	5.7e5	2.7
1800	1.1e6	5.2
2100	1.5e6	8
2400	4e6	19
2700	5e6	22
3000	7e6	28

The impact of varying speed on the electro-mechanical parameters can be attributed to fluctuations in the magnetic field's magnitude and frequency (see Table 1). The separation phenomenon is affected by the magnetic interaction between the rotating magnetic field of the separator disk and the conductive particles dipole (resulting in generating the secondary magnetic field in particles). Consequently, the relative movement of these excited non-ferrous particles within the fluctuating magnetic field leads to substantial eddy currents and repulsive forces acting on

the particles. With speed elevation, the magnetic force increased (from 1.44 to 28) 20 times for speed variation from 300 to 3 000, respectively.

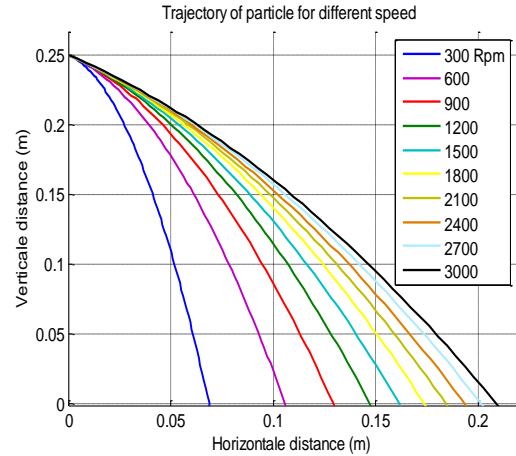


Fig. 5 – Computation of ejection distance according to speed variation.

The increasing angular velocity of the vertical disk helps improve aluminum particles' ejection distance because the induced current and, consequently, the magnetic ejection force will be significant (Figure 5). This is very important for sorting the mixture of glass and aluminum particles.

### 5. EXPERIMENT REALIZED OF INDUCTION SEPARATION DEVICE

The experiment separation process by induction separation device is shown in Fig. 6. The aim is to recover the non-ferrous particle with high purity in collector II and glass in collector I. The experimental separation results of the mixture (non-ferrous and non-metallic particles) show a high purity of particles, 100 %, in each collector because the non-ferrous particles are ejected with Lorentz force. Still, the glass particles fall under her gravity, and their weight is represented in Fig. 6.

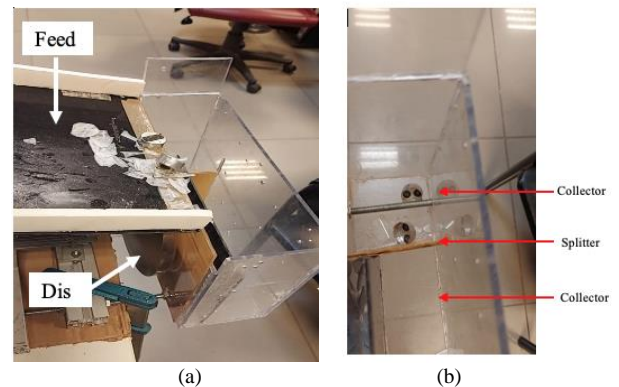


Fig. 6 – Separation setup of induction magnetic separator; a – feeder with a mixture of glass and non-ferrous particles; b – particles separation in two collectors.

Table 2

Particle separation in two collectors (%)

Speed (Rpm)	Particles			
	Collector I		Collector II	
	Glass	Aluminum	Glass	Aluminum
300	100 %	0%	0%	100 %
600	100 %	0%	0%	100 %
1200	100 %	0%	0%	100 %
1500	100 %	0%	0%	100 %
1800	100 %	0%	0%	100 %
2100	100 %	0%	0%	100 %
3000	100%	0%	0%	100 %



The separation experiment results conducted on the glass/aluminum mixture reveal that as the rotational speed of the magnetic disk increases, the totality of non-ferrous particles is propelled towards the upper level, where they are collected in the second, more distant collector. In contrast, the glass particles predominantly descend and accumulate at the lower level, first in the closer collector.

The experimental separation results show a considerable rate of separation of 100% with speed variation from 300 to 3 000 rpm because the ejection force of non-ferrous particles is more important than glass particles falling directly under her weight and gravity. Each collector contains one kind of particle with high purity; from separation results, the induction separation based on the eddy current effect is an efficient solution to recover a mixture of material from lamp neon waste (Table 2 and Fig. 6).

Table 3

Experiment and simulation results of ejection distance on non-ferrous particles

Speed (Rpm)	Particles		Error (Cm)
	Aluminum		
	Experiment	Simulation	
300	7.4	6.8	0.6
600	11	10.6	0.4
900	13.6	13	0.6
1200	15	14.7	0.3
1500	16.7	16.1	0.6
1800	17.8	17.3	0.5
2100	19	18.4	0.6
2400	20.2	19.4	0.8
2700	21	20.5	0.5
3000	24	23	1

The experimental data concerning the phenomena of separation and repulsion can be elucidated by considering the simulation outcomes that account for the impact of rotational speed on electromagnetic properties and the ejection distance. The ejection distance varies based on several parameters, such as the orientation of complexly shaped aluminum particles (in three positions on the surface or at two extremities, each characterized by different induced currents). To address this variability, we conducted multiple experimental trials to determine the optimal ejection position, which was found to be in the mean. The ejection distance exhibits a variation, transitioning from 7.4 to 24 centimeters as the rotational speed increases from 300 to 3 000 rpm respectively. All results are presented in Table 3. The convergence of ejection distances between simulation and experimental observations, with minimal errors, is effectively anticipated through numerical computational methods.

## 6. CONCLUSIONS

The primary objective of this research was to investigate the magnetic characteristics of an induction separator and analyze the induced current and ejection force in non-ferrous particles of neon lamps. This investigation used numeric simulation based on the finite element method. By utilizing the findings obtained from these simulations, we were able to provide a precise explanation of the influence of various parameters on the separation process.

The experimental results show the efficacy of the permanent magnet separator in sorting non-ferrous particles from neon lamp waste (glass and non-ferrous mixture) with a high rate of 100 % by repulsive Lorentz force, with the influence of speed rotation on ejection distance. The simulation and experiment results complement each other to explain the eddy current technique and electromagnetic

properties of the separator. The new induction separator effectively segregates waste mixtures of lamps, which include non-ferrous and non-metallic particles, yielding highly favorable separation outcomes.

Finally, applying induction magnetic separation confers numerous advantages, such as a straightforward machinery setup, a high recovery rate, efficient purification, swift separation times, economic viability, and cost-effectiveness.

## ACKNOWLEDGMENTS

The authors extend their appreciation to Taif University, Saudi Arabia, for supporting this work through the project number (TU-DSPP-2024-14). The researchers would like to acknowledge the Deanship of Scientific Research to the MAGLEV laboratory staff at Yildiz University in Istanbul, Turkey. They provided invaluable assistance during a short internship and played a crucial role in helping with technical materials and the successful implementation of the new experiment separator.

Received on 30 September 2023

## REFERENCE

1. D. Gaitanelis, D. Logothetis, G. Perkoulidis, N. Moussiopoulos, *Investigation and evaluation of methods for the reuse of glass from lamps recycling*, J. of Cleaner Production, **172**, 3, pp.1163–1168 (2018).
2. D.M. Rahman, S. Pompidou, T. Alix, B. Laratte, *A review of LED lamp recycling process from the 10 R strategy perspective*, Sustainable Production and Consumption, **28**, pp.1178–1191 (2021).
3. C.J. Grigoropoulos, L.T. Doulos, S.C. Zerefos, A. Tsangrassoulis, P. Bhusal, *Estimating the benefits of increasing the recycling rate of lamps from the domestic sector: Methodology, opportunities and case study*, Waste Management, **10**, 1, pp. 188–199 (2019).
4. L. Benmamas, Y. Bouzidi, G. Housset, K. Nomenyo, K. Bru, M. Beaulieu, P. Leclere, L. Clerget, G. Lerondel, *Selective separation of plastic LED lamp components using electrodynamic fragmentation for material recovery*, Waste Management, **144**, 4, pp. 210–220 (2022).
5. R.S. York, J.R. Nagel, R.K. Rajamani, *Eddy current separation for recovery of non-ferrous metallic particles: A comprehensive review*, Minerals Engineering, **133**, pp. 149–159 (2019).
6. M. Lungu, P. Rem, *Eddy-current separation of small non-ferrous particles by a single-disk separator with permanent magnets*, IEEE Transactions on Magnetics, **39**, 4, pp. 2062–2067 (2003).
7. A.N.I. Ayad, A. Ayad, Y. Ramdani, *Simulation of eddy current separation of gold particles from sands*, International Journal of Engineering and Manufacturing (IJEM), **6**, 5, pp. 30–37 (2016).
8. A.N.I. Ayad, M. Larab, H. Boudjella, F. Benhamida et al., *Simulation of eddy current and repulsive force of non-ferrous particles in eddy current separator*, Przeglad Elektrotechniczny, **95**, 6, pp. 49–54 (2019).
9. M. Ouili et al., *A simultaneous separation of magnetic and conductive particles in a designed permanent magnet drum separator*, IOS Press, **61**, 1, pp. 137–155 (2019).
10. I. Dobrin, D. Enache, G. Dumitru, M. Gutu, S. Zamfir, R. Pinte, *Curved dipolar electromagnet, numerical modeling and design*, Rev. Roum. Sci. Techn.–Électrotechn. et Énerg., **67**, 4, pp. 409–415 (2022).
11. M. Ouili et al., *Coupling of PSO and FE methods for electrical conductivity identification of materials used in eddy current separator*, **72**, 2, pp. 100–114 (2023).
12. A.N.I. Ayad, *Etude et réalisation d'un séparateur à induction électromagnétique*, Thesis, Djilali Liabes University Sidid Bel Abbes, Algeria (2017).
13. N. Dholu, J.R. Nagel, D. Cohrs, R.K. Rajamani, *Eddy current separation of non-ferrous metals using a variable-frequency electromagnet*, KONA Powder and Particle Journal, **34**, 12, pp. 1–7 (2016).
14. N. Bin, Y. Yi, S. Zhicheng, W. Qiang, A. Abdelkader, A. Kamali, D. Montalva, *Effects of particle size on the separation efficiency in a rotary-drum eddy current separator*, Powder Technology, **410**, pp.1–35 (2022).